

PROCEEDINGS OF SPIE

SPIDigitalLibrary.org/conference-proceedings-of-spie

Impact localization on composite plates using two developed imaging methods

Migot, Asaad, Bhuiyan, Yeasin, Giurgiutiu, Victor

Asaad Migot, Yeasin Bhuiyan, Victor Giurgiutiu, "Impact localization on composite plates using two developed imaging methods," Proc. SPIE 11376, Active and Passive Smart Structures and Integrated Systems IX, 113760V (22 April 2020); doi: 10.1117/12.2558277

SPIE.

Event: SPIE Smart Structures + Nondestructive Evaluation, 2020, Online Only, California, United States

Impact localization on composite plates using two developed imaging methods

Asaad Migot^{*1, 2}, Yeasin Bhuiyan³, Victor Giurgiutiu²

¹Department of Mechanical Engineering, Thi-Qar University, Iraq

²University of South Carolina, Columbia, SC, USA

³Collins Aerospace, Vergennes, VT, USA

*Corresponding author: migotasaad@gmail.com

ABSTRACT

This paper focuses on using two developed imaging methods to localize the impact points on a composite plate. The first developed imaging method (Method 1) was firstly investigated on a metallic plate. A network of nine piezoelectric wafer active sensors (PWAS) was instrumented on an aluminum plate to receive impact signals. Based on Method 1, we need at least three sensors, which can be used to determine two hyperbolic paths, to localize an impact point on a metallic plate with known group velocities of generated waves (known its material properties). The observed results indicate that Method 1 can be used successfully to localize the impact points on a metallic plate. These successful results motivated us to investigate Method 1 on a composite plate. A second experiment of impact localization was implemented on a composite plate. Two clusters of sensors (every cluster has three PWAS transducers) were instrumented on the composite specimen to receive the generated acoustic waves due to break pencil leads at different points. The received signals were analyzed using a wavelet transform to determine the time of flight. The group velocity profile of antisymmetric Lamb wave mode was determined analytically at certain frequency. Based on Method 1, two hyperbolic paths, which are generated by four sensors, can be used successfully to localize the impact points on a composite plate with known its material properties. The second developed imaging method (Method 2) was investigated on the same composite specimen with assumption of unknown its material properties (unknown group velocity profile of generated wave). Based on Method 2, we need six sensors distributed on two clusters to determine two straight line paths. The intersection point of these two lines represents the impact point. The results showed that Method 2 can successfully localize the impact points on a composite plate.

Keywords: impact localization, imaging methods, Lamb waves, group velocity profile, piezoelectric wafer active sensors

1. INTRODUCTION

Composite materials are being the major component in aerospace structures due to the advantages of their properties (e.g., high strength and stiffness and light weight)^{1, 2}. Unlike metallic materials, the anisotropic behavior of composite material makes the process of detecting and localizing the structural damages more difficult³. The successful works related to quantifying damages in composite structures are always challenging⁴. Many researches have been implemented in the scope of using SHM systems to investigate and localize damages and impact events on aerospace structures^{5, 6}. The aerospace structure, which is hit by a forging object, may have a visible or invisible damage⁷. The composite structural defects (e.g., delamination, matrix cracking and fiber breakage) can generate acoustic waves⁸. These acoustic waves can be received by passive sensors. The Piezoelectric wafer active sensor (PWAS), which has low cost and light weight, can be used for passive sensing of acoustic waves⁹. It can be easily to install it on inspected structure to monitor the structural health status and quantify structural damages. The passive systems are able to localize the impact points by installing ultrasonic sensors on the structure surface to receive the generated signals of internal or external sources. The PWAS transducers have been used in various application such as impact localization and damage detection and quantification in metallic and composite plates^{10, 11, 12}. Numerical methods were used for impact or damage localization using several networks of sensors. The results showed that the errors of localizing impact points decrease with increasing the number of used sensors¹³. The acoustic emission (AE) caused by the growth of the fatigue crack was studied extensively using the physics based approach¹⁴. A new linear technique is developed to localize the acoustic source in anisotropic plate without knowing the direction dependent velocity profile using six sensors, which are distributed in two clusters¹⁵. For in situ SHM, a new system was developed to localize the AE sources in anisotropic structure. The coordinate location of impact events

are determined by solving a set of nonlinear equations¹⁶. In recent years, some imaging methods have been used sufficiently to localize and size different kinds of aerospace structural defects. These methods are based on guided Lamb waves and sensors network^{17,18,19,20,21}. In this paper, we developed two imaging methods to localize the impact events on metallic and composite plates based on received impact signals.

2. DEVELOPED IMAGING METHODS FOR IMPACT LOCALIZATION

Two developed imaging methods were used to localize low velocity impact events. These methods are based on received acoustic signals. The idea of using imaging methods for localizing structural defects or acoustic emission sources is to determine the defect orbits (paths). The defect path can be defined using ellipse, circle, hyperbola, or slope equations. The intersection of at least two paths (hyperbola or straight paths) or at least three paths (ellipse or circle paths) gives the defect or the acoustic emission source location. Two developed imaging methods (Method 1 and Method 2) were used in this work. Method 1 can be used to localize the impact events on structural like plate with known its material properties. Method 2 can be used for structural like plate with unknown its material properties.

2.1 Method 1

This method involved impact signals and Gaussian distribution function. The interested area is divided into pixels as shown in Figure 1. In order to investigate the interested area pixels whether have impact source or not, we have to determine the difference in time of flight of two impact signals received by two sensors at every pixel using the following hyperbola equation¹⁹

$$\Delta t_{ij} = \frac{\sqrt{(x_1 - x_i)^2 + (y_1 - y_j)^2}}{v_g} - \frac{\sqrt{(x_1 - x_2)^2 + (y_1 - y_2)^2}}{v_g} \quad (1)$$

where Δt_{ij} is the difference in time of flight of the signals received by sensors #1 and #2 when the impact point at pixel $P(x, y)$, $x_1, y_1, x_2, y_2, x_i, y_j$ are the coordinates of sensors #1 and #2, and pixels, respectively, v_g is the group velocity of Lamb wave mode. When the pixels lay on the impact source orbit of a particular sensing path then, $\Delta t_{ij} = \Delta t_{12}$.

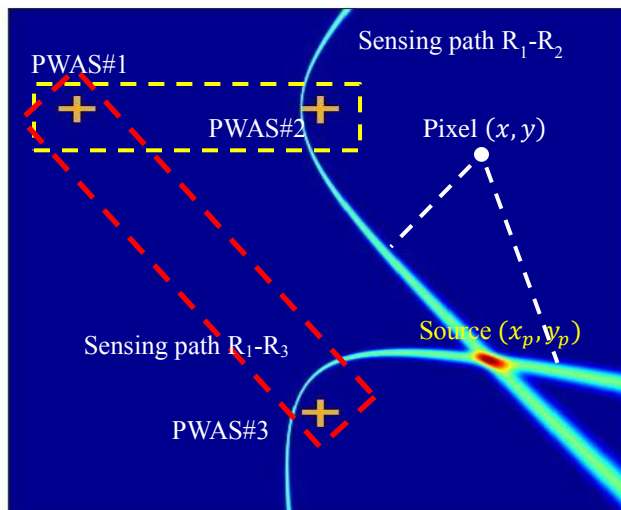


Figure 1. Imaging concept of Method 1 for localization an impact point.

The field value of each pixel is determined by using the Gaussian distribution function¹⁹. The equation of Gaussian distribution function is given below:

$$f_{ij}^k(x, y) = \frac{1}{\sigma\sqrt{2\pi}} e^{-\frac{(x-\mu)^2}{2\sigma^2}} \quad (2)$$

where $f_{ij}^k(x, y)$ is the field value of every pixel $P(x, y)$ of the sub-image of a particular sensing path, x represents the difference time of flight at each pixel point $(\Delta t_{ij}(x, y))$, which is determined using Eq. (1), for a particular sensing path $R_m - R_{m+1}$, μ represents the experimental value of difference in time of flight between two impact signals received by sensors R_m, R_{m+1} . The standard deviation, σ which describes the variability or dispersion of a data set, which was taken as half of the time range of wave packet.

To fuse all the sub-images of different sensing paths, summation and/or multiplication algorithm were used⁶, following the equations below:

$$\begin{aligned} P_{sum}(x, y) &= \sum_{k=1}^N f_{ij}^k(x, y) \\ P_{mult}(x, y) &= \prod_{k=1}^N f_{ij}^k(x, y) \end{aligned} \quad (3)$$

where $P_{sum}(x, y), P_{mult}(x, y)$ are the total field values of each pixel point using summation or multiplication algorithm and N represents the total number of sensing paths, i.e.,

$$N = N_R! / (2!(N_R - 2)!) \quad (4)$$

where N_R is the total number of used sensors. Figure 1 shows the image of localization an impact event. In this image, we used summation algorithm to fuse two sub-images of sensing paths $R_1 - R_2$ and $R_1 - R_3$. The intersection of these two paths (the pixel with maximum field value) gives the location of an impact point.

2.2 Method 2

This method can be used to localize the defects or impact events on composite plates based on time of flight (TOF) of received signals and slope equations. Two clusters of sensors (every cluster has three sensors) were used to receive impact signals as shown in Figure 2. In this method, we do two steps to localize an impact point on the interested area. In First step, we determine the experimental slope values for every cluster based on the time of flight of impact signal¹⁵

$$\begin{aligned} \text{Slope}^1 &= \frac{\Delta t_{23}}{\Delta t_{21}} \\ \text{Slope}^2 &= \frac{\Delta t_{56}}{\Delta t_{54}} \end{aligned} \quad (5)$$

where Δt_{23} represents the difference in time of flight of impact signals received by sensors S_2 and S_3 .

In the second step, we divided the inspected area into small pixels. The slope values for every pixel for a particular sensing path line of a particular cluster can be determined using Eq. (6).

$$\begin{aligned} \text{Slope}_{ij}^1(x, y) &= \frac{y_2 - y_i}{x_2 - x_j} \\ \text{Slope}_{ij}^2(x, y) &= \frac{y_5 - y_i}{x_5 - x_j} \end{aligned} \quad (6)$$

where $(x_2, y_2), (x_5, y_5)$ are the coordinates of sensors S_2 (Cluster 1) and S_5 (Cluster 2) respectively. To determine the pixels field values of a sub-image of a particular sensing path, we use Gaussian distribution equation (Eq. (2)). In this equation, $f_{ij}^k(x, y)$ represents the field value of every pixel image of a particular sensing path (for a particular cluster), x represents the slope value at each pixel for a particular sensing path of a Cluster k , μ represents the experimental slope value for a sensing line path of Cluster k which can be determined using Eq (5). The standard deviation, σ which describes the variability or dispersion of a data set, which was taken as function of slope value. In this work, the σ values were taken between 0.02–1 (the σ value needs to be increased with increasing slope value and vice versa), k represents the order of used cluster.

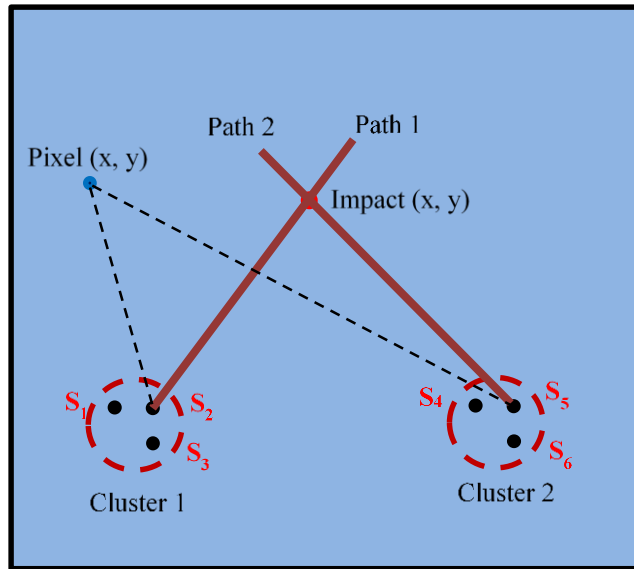


Figure 2. Imaging concept of Method 2 for localization an impact point¹².

3. EXPERIMENTAL SETUP AND SIGNAL ANALYSIS

Two impact experiments were implemented to localize impact events on metallic and composite plates. In first experiment, an aluminum plate, has dimensions 914 mm in length, 503 mm in width and 1mm in thickness, was instrumented with a network of nine PWAS transducers. This plate was subjected to impacts by a small steel ball (0.33 g), it was dropped from a height of 50 mm through a small plastic pipe, at three different locations (they marked as #1, #2 and #3).

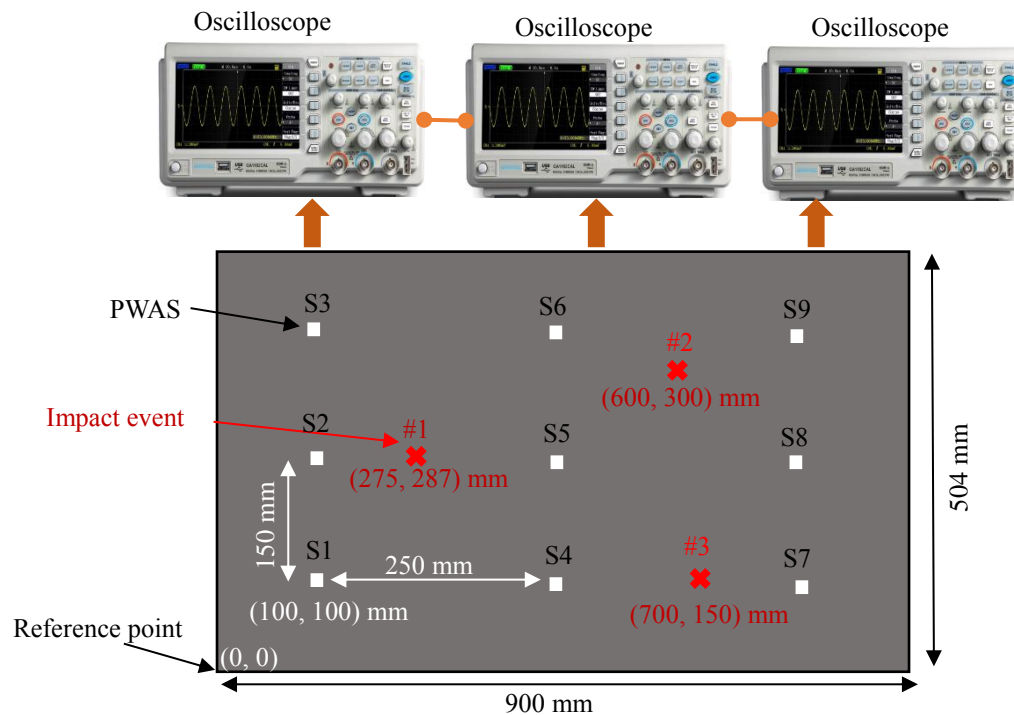


Figure 3. Experimental setup of impact localization on an aluminum plate.

The generated impact signals were received by a network of nine PWAS transducers and recorded by three Oscilloscopes. The experimental setup, instrumented sensors and the location of impact points are shown in the Figure 3. The nine signals received by nine sensors, which correspond to the impact at location #1, are observed in Figure 4a. To get accurate values of time of flight (TOF), the signal processing methods should be used. In this work, we used wavelet transform based signal processing method to determine the TOF. Figure 4b shows the wavelet transform of analysis window part of impact signal (the impact event is at location #1) received by sensor S1. In this figure, the frequency-time is shown by the color plots. It shows the amplitude mapping over various frequencies and time. At each time and frequency, a WT coefficient variation can be plotted as shown on the bottom-left of box. An overall maxima of the WT coefficient has been plotted. The time at which the WT profile matches the overall WT maxima provide the TOF (the time at maximum signal amplitude). The Continuous Wavelet Transform (CWT) of the signals are determined with AGU-Vallen Wavelet, a freeware software program²². This program has a Gabor function as the “mother” wavelet. The second impact experiment was implemented on a composite plate to predict the location of impact events by pencil lead breaks. In this experiment, 5-Harness woven thermoplastic composite plate with dimension 0.3 m × 0.3 m × 0.001 m instrumented with six PWAS transducers. These sensors are distributed in two clusters (Cluster 1 at coordinate location (30, 150) and Cluster 2 at location coordinate (120, 30)). Each cluster has three PWAS transducers placed at 90 deg. orientation. The configuration of sensors was chosen based on Kund et al work (2014). The impact signals are received by

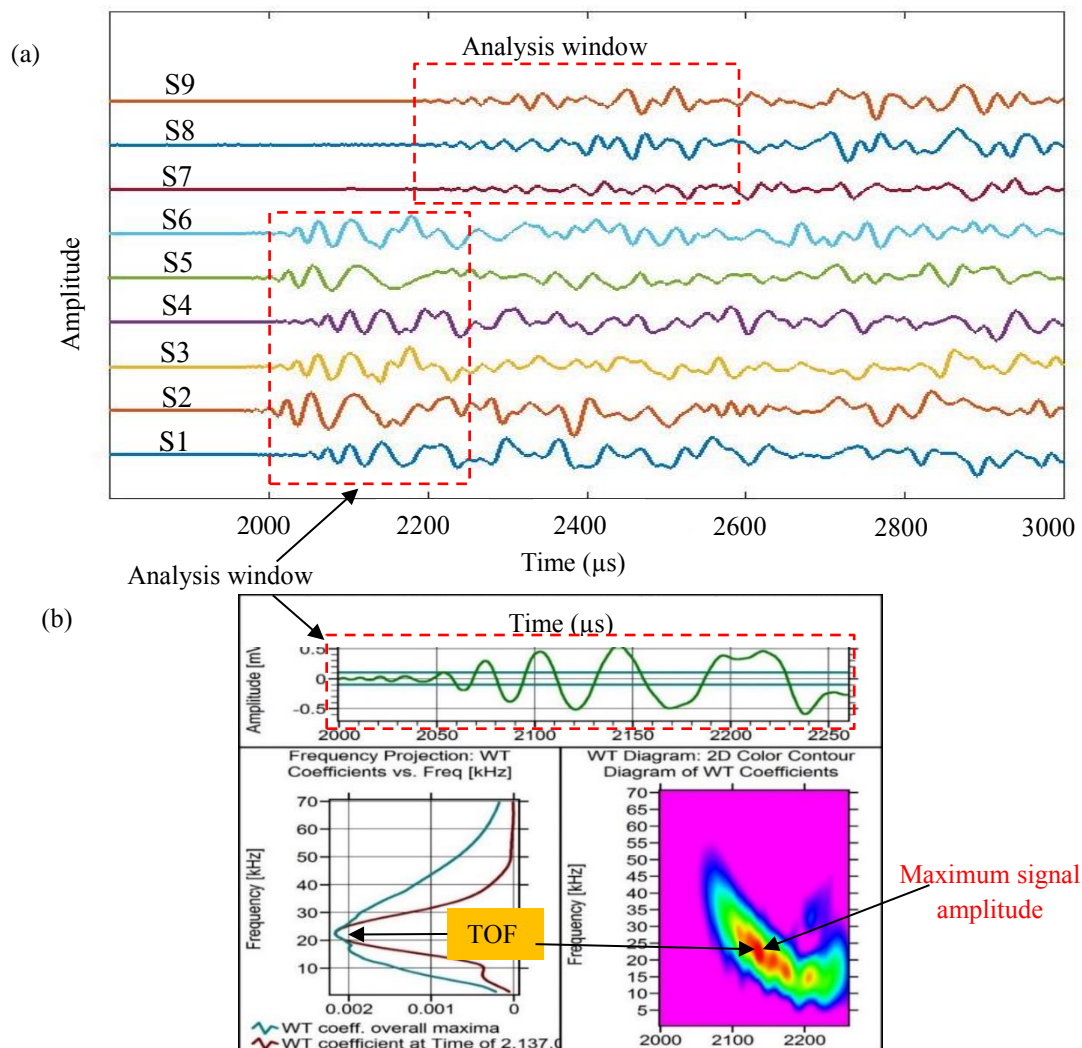


Figure 4: (a) The time domain of nine impact signals received by nine PWAS transducers due to impact on the aluminum plate at point #1(275, 287) mm; (b) Wavelet transform of the signal received by sensor S1.

these six sensors and recorded by two oscilloscopes. The five impact points were marked by #1, #2, #3, #4, and #5. All the details of the experimental setup are observed in Figure 5.

The TOF of the received signals were determined at maximum signal amplitude (energy). The CWT plot is very helpful to determine the features of a signal (time of flight (TOF), frequency, and amplitude). Based on the CWT plot, The TOF is determined at maximum wavelet coefficient which is at frequency around to 30 kHz. The time domains of six acoustic wave signals due to pencil lead break at point #1 are shown in Figure 6a. The wavelet transform was used for all received signals through six PWAS transducers. The wavelet transform of the signal received by sensor S_2 can be observed in Figure 6b. After time estimation of all generated signals due to impact events, the impact events were localized using developed imaging methods (Method 1 and Method 2).

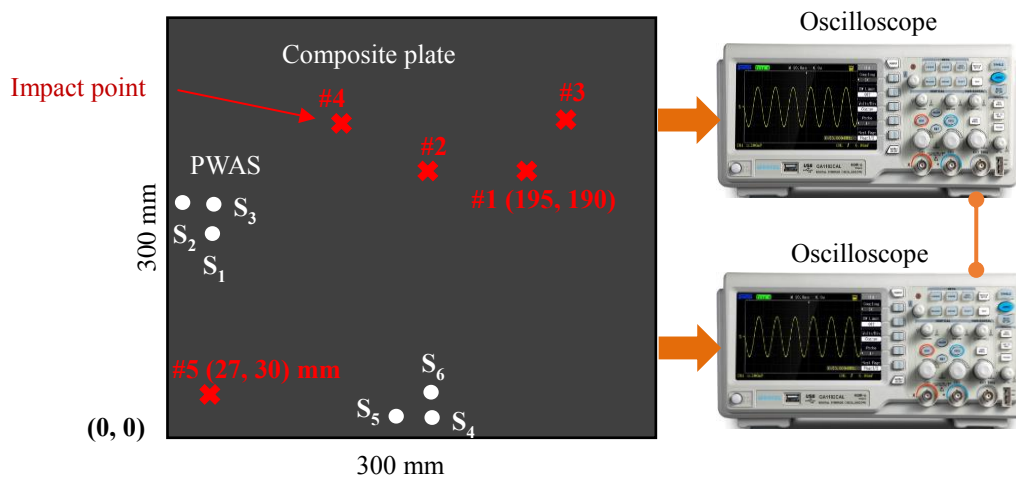


Figure 5. Experimental setup of impact localization on the composite specimen.

4. IMPACT LOCALIZATION RESULTS

4.1 Results of Method 1

After estimation TOF of all received signals, the developed imaging Method 1 was used to localize the impact events on metallic and composite specimens. For the first experiment of metallic plate, the group velocity of propagating waves, which is determined analytically at frequency 22 kHz, represents the group velocity of antisymmetric Lamb wave mode (A0). Based on Method 1, three sensors can be used successfully to localize the impact point on the metallic plate using hyperbolic paths. In Figure 7a, three hyperbolic paths, generated by three sensors, can successfully localize the impact event at location #1. The result of localization the impact events becomes much better with increasing the number of used sensors as demonstrated in Figure 7b. The imaging results of localization the impact events #2 and #3 are shown in Figure 8. From these results, it can be observed that the measured impact locations are in good agreement with the actual impact locations.

After getting acceptable results of localization impact events on metallic plate, the Method 1 was used to localize the impact events on the composite plate. Unlike metallic plate, the group velocities of propagating waves in a composite plate are directional dependent. Before using Method 1, the direction-dependent group velocity profile was determined analytically for the interested composite specimen based on its material properties. In this experiment, because we have low velocity impact events, the antisymmetric Lamb wave mode (A0) is clearly apparent in the received signals. Four sensors, distributed in two cluster as shown in Fig 9, were used with Method 1 to localize the impact events. We assume the two sensors in one cluster have the same group velocity value. To determine the group velocity value for every cluster, we need to predict the location of impact source on the interested area.

A simple method was developed to estimate approximate group velocity values of propagating waves based on the location of the used four sensors and TOF of received signals. In this method, the impact point can be indicated in one of nine locations on the interested area based on the TOF values of four received signals. For example, when the t_{S1} (TOF of

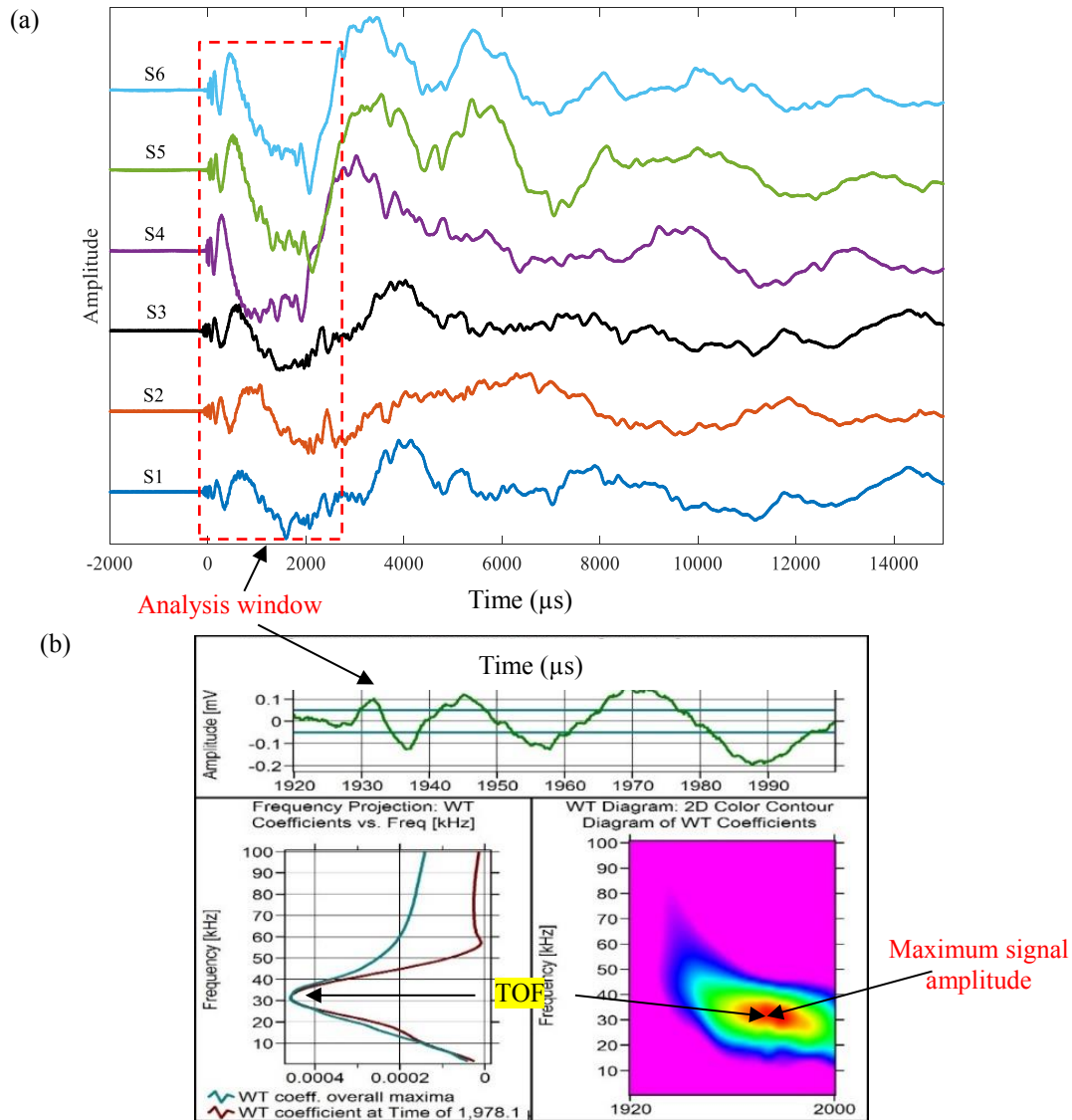


Figure 6. (a) The time domain of six impact signals received by six PWAS transducers due to impact on the composite specimen at point #1(195, 190) mm; (b) Wavelet transform of the signal received by sensor S₂.

sensor S₁) is larger than t_{S2} (TOF of sensor S₂) and t_{S4} is larger than t_{S3} . Based on these relations, the impact point can be indicated at location #7 as shown in Figure 9. When the sensors S₁ and S₂ have the same TOF values and S₃ and S₄ have the same TOF values, the impact point can be indicated at location #5.

After indicating the location of impact point as shown in Figure 10a, The direction of generated waves, which are received by sensors can be identified. Based on the direction of generated waves, their group velocity values can be determined using the group velocity profile of A0 mode which is shown in Figure 10b. The group velocity profile of A0 mode was determined at frequency 30 kHz. Based on wavelet transform contour, the frequency value is chosen at the maximum wavelet coefficient of received signals.

Increasing the number of used sensors helps to divide the interested area into small segments and to get accurate group velocity values of propagating waves. Once the TOF and the group velocities of generated waves are determined, the developed imaging Method 1 can be used to localize the impact events. Figure 11 illustrates the imaging results of localization the impact points #1 and #5. In Figure 11a, c, we used summation algorithm for data fusion while in Figure 11b, d, we used multiplication algorithm to fuse all imaging data. The measured and actual coordinates of impact events

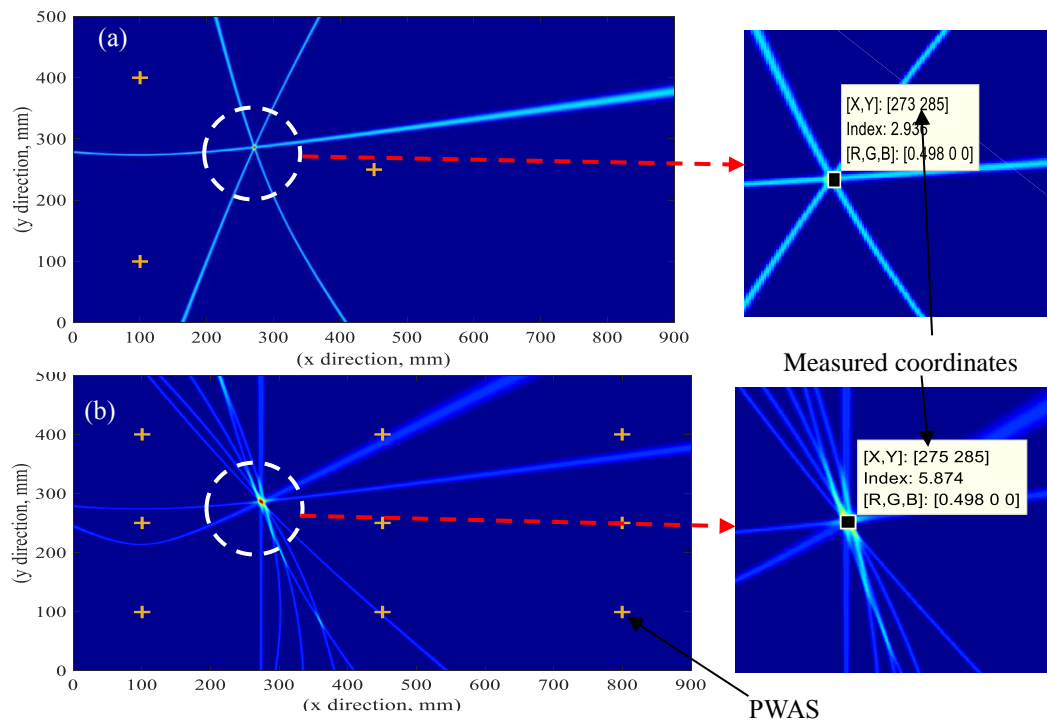


Figure 7: Imaging results of localization impact point #1(275, 287) mm using different number of used sensors: (a) 3 used sensors; (b) 9 used sensors.

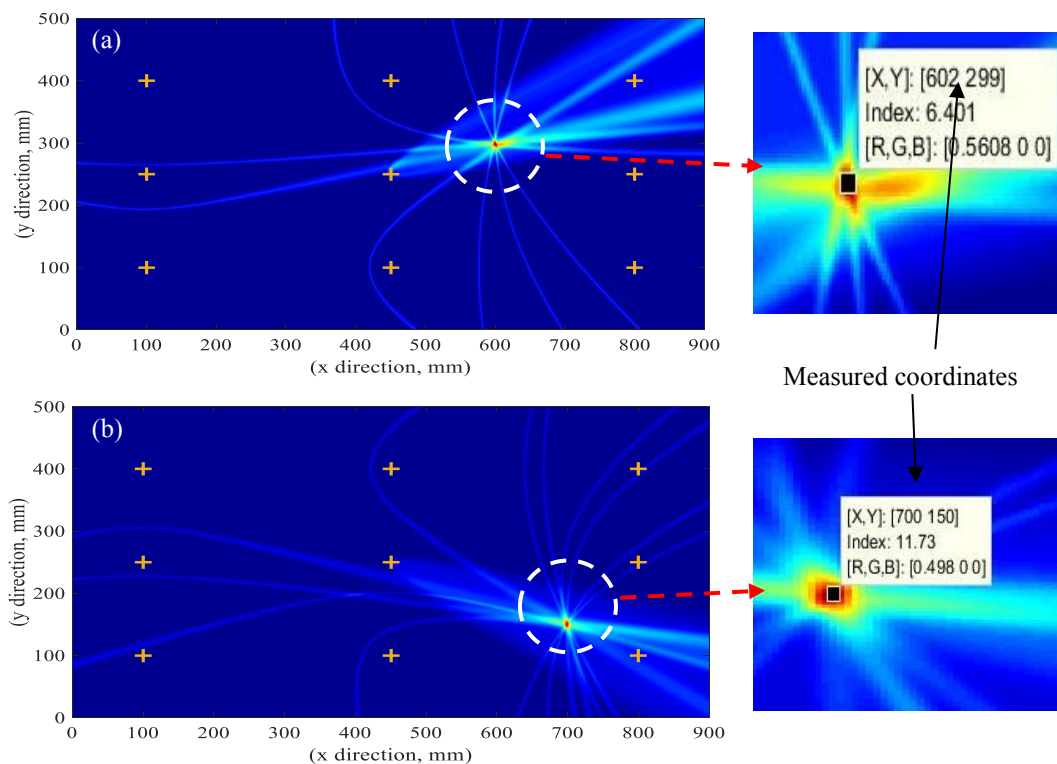


Figure 8: Imaging results of localization the impact events: (a) #2(600, 300) mm; (b) #3(700, 150) mm.

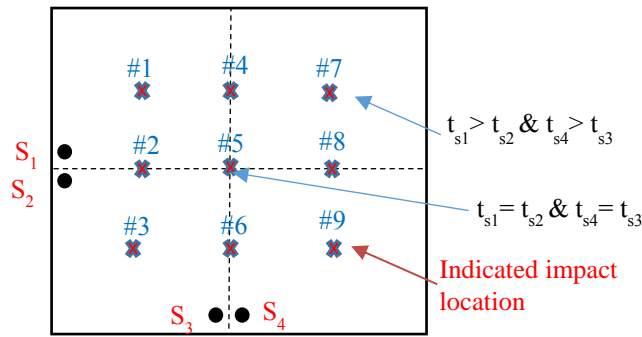


Figure 9. Simple method of indicating the impact location in nine locations based on the time of flight of received signals

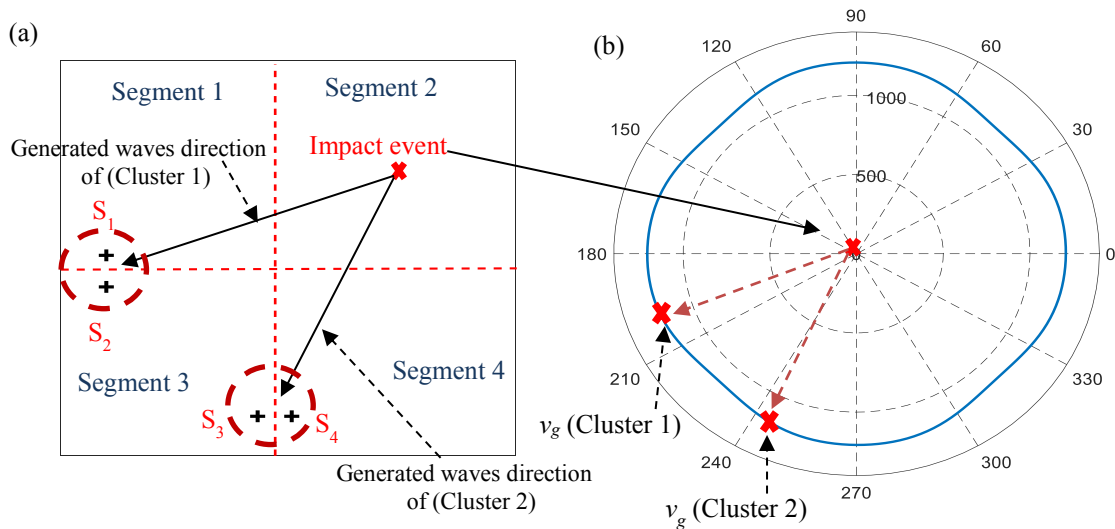


Figure 10. Estimating of group velocities values of received signals due to impact at point #1 (195, 190) mm: (a) identifying the generated waves direction; (b) Analytical group velocity profile of A0 mode at frequency 30 kHz.

are listed in the Table 1. The location error was determined for every measured impact event by following the equation in our previous work¹². The result shows that the measured impact points determined by Method 1 are in good agreement with the actual impact points. The location errors are due to errors in determination of the group velocity values and time of flight of received signals.

Table 1: Experimental measurement of Method 1 and actual location of five impact events.

Impact events	Actual location (x, y) mm	Measured location (x, y) mm	Location error (mm)
#1	(195, 190)	(191, 187)	5
#2	(155, 190)	(160, 187)	5.8
#3	(255, 230)	(253, 233)	3.6
#4	(135, 230)	(134, 228)	2.25
#5	(27, 30)	(30, 30))	3

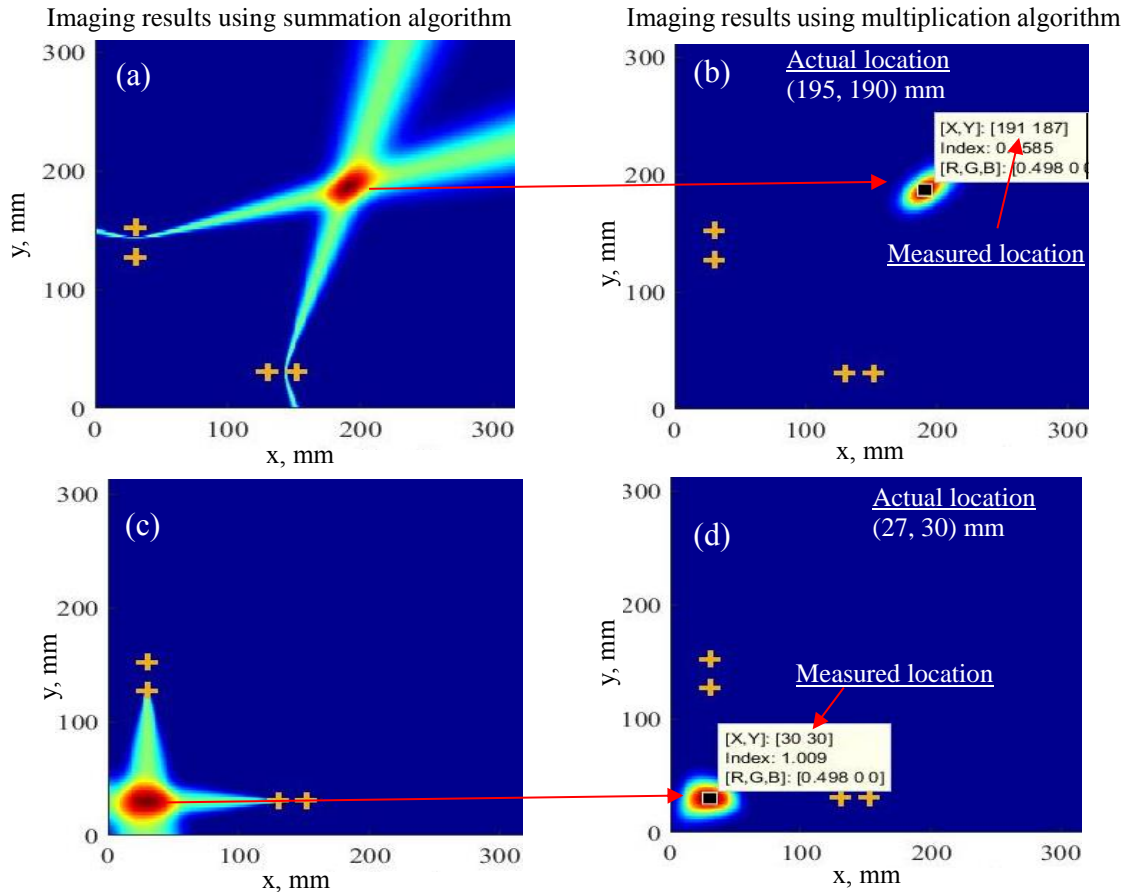


Figure 11. Imaging results of impact localization on composite specimen using Method 1: (a) and (b) impact point #1(195,190) mm; (c) and (d) impact point #5 (27, 30) mm.

4.2 Results of Method 2

The idea of Method 2 is to generate at least two straight paths using imaging methods. The intersection of these two paths gives the impact point location. This method is independent with the group velocity of propagating waves as mentioned in section 2.2. The experimental slope values, which are essential for Method 2, were determined from the time of flight of six received signals (Eq. (5)). Figure 12 shows the imaging results of localization impact events #1 and #3. From these images, we can observe two straight paths come from two clusters and intersect at the location of impact events #1 and #3. The measured and actual impact points are summarized in Table 2. From this table, It can be observed that the results of

Table 2. Experimental measurement of Method 2 and actual location of five impact events.

Impact events	Actual location (x, y) mm	Measured location (x, y) mm	Location error (mm)
#1	(195, 190)	(194, 188)	2.25
#2	(155, 190)	(154, 188)	2.25
#3	(255, 230)	(258, 229)	3.2
#4	(135, 230)	(134, 229)	1.4
#5	(27, 30)	(26, 29)	1.4

localization the impact events using Method 2 are very accurate compared with actual impact location. Based on the measured results of Table 1 and Table 2, we can observe that the results of Method 2 much accurate than Method 1 because Method 2 independent with group velocity profile of propagating waves while Method 1 needs the group velocity profile of propagating waves to localize impact events.

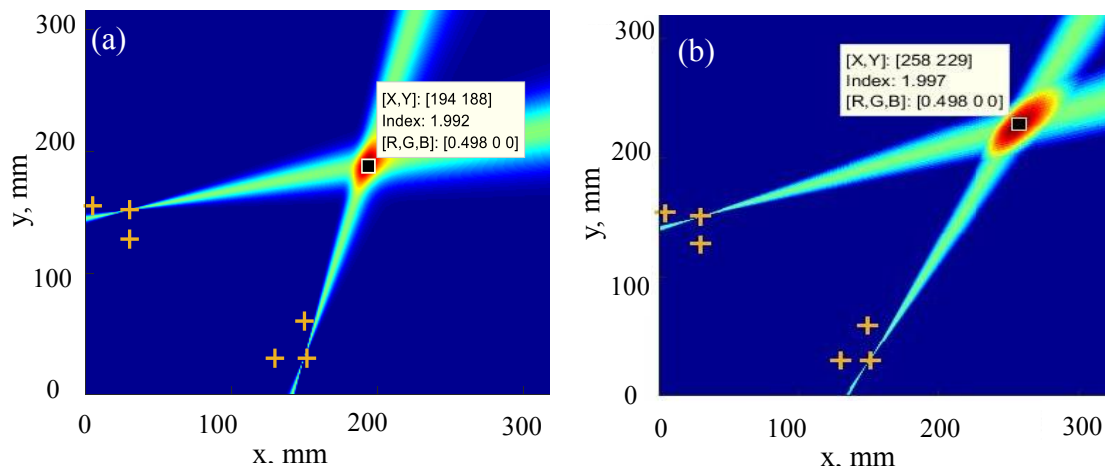


Figure 12. Imaging results of developed Method 2 for localizing impact events on composite plate: (a) impact event #1 (195,190); (b) impact event #3 (255, 230).

5. CONCLUSION

Piezoelectric wafer active sensors can successfully be used to monitor metallic and composite structures. The wavelet transform represent a powerful signal processing method to estimate the time of flight of acoustic signals. Two developed imaging methods can successfully be used for localizing the impact events on composite structures. The developed imaging Method 1 can accurately localize the impact events on metallic and composite plates with known their material properties. The composite structure with unknown its material properties can be successfully monitored in practice using developed imaging Method 2. Both developed imaging methods come up with acceptable results of impact localization compared with actual impact locations. The results of Method 2 much accurate than results of Method 1. The result of localization the impact events on the metallic plate becomes much better with increasing the number of used sensors.

ACKNOWLEDGEMENTS

This study was supported by Iraqi Ministry of Higher Education and Laboratory for Active Materials and Smart Structures (LAMSS), which is thankfully acknowledged.

REFERENCES

- [1] Coelho, C. K.; Hiche, C. and Chattopadhyay, A., "Impact Localization and Force Estimation on a Composite Wing using Fiber Bragg Gratings Sensors," *Proc. AIAA/ASME/ASCE/AHS/ASC Structures* 2905, 2010.
- [2] Park, W. H.; Packo, P. and Kundu, T., "Acoustic source localization in an anisotropic plate without knowing its material properties: a new approach," *Ultrasonics*, Vol. 85, 9-17, 2016.
- [3] Mei, H. and Giurgiutiu, V., "Wave damage interaction in metals and composites," *Proc. SPIE* 10972, Health Monitoring of Structural and Biological Systems XIII, 109720O, 2019.
- [4] Wang, D.; Ye, L.; Lu, Y. and Su, Z., "Probability of the presence of damage estimated from an active sensor network in a composite panel of multiple stiffeners," *Composites Science and Technology*, vol. 69, 2054–2063, 2009.
- [5] Yu, L. and Giurgiutiu, V., "Piezoelectric Wafer Active Sensor Guided Wave Imaging," *Proc of 2010 SPIE*, vol. 7648,

pp 1–11, 2010.

- [6] Migot, A.; Bhuiyan, Y. and Giurgiutiu, V. “Numerical and experimental investigation of damage severity estimation using Lamb wave-based imaging methods,” *Journal of Intelligent Material Systems and Structures*, vol. 30, no. 4, 618–635, 2019.
- [7] Shrestha, P.; Kim, J. H.; Park, Y. and Kim, C. G. (2015) “Impact localization on composite wing using 1D array FBG sensor and RMS/correlation based reference database algorithm,” *Composite Structures*, vol. 125, pp. 159–169, 2015.
- [8] Si, L. and Baier, H. “Real-Time Impact Visualization Inspection of Aerospace Composite Structures with Distributed Sensors,” *Sensors*, vol. 15, pp. 16536–16556, 2015.
- [9] Mei, H.; Haider, M. F.; Joseph, R. and Migot, A. “Recent Advances in Piezoelectric Wafer Active,” *Sensors*, vol. 19, no. 2, p. 383, 2019.
- [10] Wang, C. H.; Rose, J. T. and Chang, F.-K. “A synthetic time-reversal imaging method for structural health monitoring,” *Smart Materials and Structures*, vol. 13, no. 2, pp. 415–423, 2004.
- [11] Yu, L. and Giurgiutiu, V. “In situ 2-D piezoelectric wafer active sensors arrays for guided wave damage detection,” *Ultrasonics*, vol. 48, no. 2, pp. 117–134, 2008.
- [12] Haider, M. F.; Migot, A.; Bhuiyan, Y. and Giurgiutiu, V. “Experimental Investigation of Impact Localization in Composite Plate Using Newly Developed,” *Inventions*, 3(3), 59, 2018.
- [13] Migot, A. and Giurgiutiu, V. (2017) “Impact localization using sparse PWAS networks and wavelet transform,” *Proc. 11th International Workshop on Structural Health Monitoring*, pp. 391–398, 2017.
- [14] Bhuiyan, M. Y.; Bao, J.; Poddar, B. and Giurgiutiu, V. “Toward identifying crack-length-related resonances in acoustic emission waveforms for structural health monitoring applications,” *Structural Health Monitoring*, Vol 17, Issue 3, 2018.
- [15] Kundu, T. “Acoustic source localization,” *Ultrasonics*, vol. 54, no. 1, pp. 25–38, 2014.
- [16] Ciampa, F. and Meo, M. “A new algorithm for acoustic emission localization and flexural group velocity determination in anisotropic structures,” *Composites Part A: Applied Science and Manufacturing*, vol. 41, no. 12, pp. 1777–1786, 2010.
- [17] Zhou, C.; Su, Z. and Cheng, L. “Quantitative evaluation of orientation-specific damage using elastic waves and probability-based diagnostic imaging,” *Mechanical Systems and Signal Processing*, vol. 25, no. 6, pp. 2135–2156, 2011.
- [18] Liu, Z.; Zhong, X.; Dong, T.; He, C. and Wu, B. “Delamination detection in composite plates by synthesizing time-reversed Lamb waves and a modified damage imaging algorithm based on RAPID,” *Struct. Control Health Monit.*, 24:e1919., pp. 1–17, 2017.
- [19] Su, Zhongqing and Ye, Lin [Identification of Damage Using Lamb Waves], *Springer-Verlag Berlin Heidelberg*, 2009.
- [20] Zhou, C.; Su, Z. and Cheng, L. (“Quantitative evaluation of orientation-specific damage using elastic waves and probability-based diagnostic imaging,” *Mechanical Systems and Signal Processing*, vol. 25, no. 6, pp. 2135–2156, 2011.
- [21] Yu, L. and Leckey, C. A. C. (2013) “Lamb wave-based quantitative crack detection using a focusing array algorithm,” *Journal of Intelligent Material Systems and Structures*, vol. 24, no. 9, pp. 1138–1152, 2013.
- [22] Vallen-System, GmbH. Munich, Germany. 2001. Available online: <http://www.vallen.de/wavelet/index.html> (accessed on 24 August 2018).